J. Chem. Sci. (2026)138:30
https://doi.org/10.1007/s12039-026-02483-1

RESEARCH ARTICLE

A helium nanodroplets isolation spectrometer for high-resolution infrared spectroscopy of cold molecules and molecular aggregates

DEVENDRA MANI*, RIYA GUPTA†, SUJAN SINGHA†, YASHIKA, POOJA RANI and POOJA KUMARI

Department of Chemistry, Indian Institute of Technology Kanpur, Kanpur 208 016, India
*Corresponding Author: [dmani@iitk.ac.in]

†These authors contributed equally to this work.

MS received 7 September 2025; revised 8 December 2025; accepted 26 December 2025

Abstract. A helium nanodroplets isolation spectrometer has been fabricated at IIT Kanpur (HeNDI-IITK) for investigating molecules, molecular clusters and chemical reactions at ultracold temperatures. To the best of our knowledge, this is the first HeNDI spectrometer developed in India and one of only a few worldwide. The spectrometer facilitates the formation and isolation of molecular clusters within superfluid helium droplets, which can then be investigated using mass spectrometry and mass-selective infrared spectroscopy. Currently, the spectrometer can perform mass spectrometry in the range of m/z =2–510 u and infrared spectroscopy in the range of 2500–4500 cm^{-1} with a high spectral resolution of 0.0001 cm^{-1}, offering potential for extending both measurement ranges in future developments. In this article, we discuss the design and performance of the spectrometer. Mass-selective infrared spectrum of formic acid monomer in the frequency range of ~3568.8–3572.7 cm^{-1} is also reported.

Keywords. Helium droplets; cold molecules; infrared spectroscopy; high-resolution spectroscopy; formic acid; mass-selective infrared spectrum.

1. Introduction

Helium nanodroplets are an ideal medium for studying isolated molecules, molecular clusters and chemical reactions at the microscopic level.[1–33] These droplets are clusters of helium atoms, formed as a result of a supersonic expansion of ultracold helium gas (99.9999% purity) from a temperature of typically 4–25 K (T_0) and a pressure of 10–80 bar (P_0). Depending on the initial expansion conditions (T_0 and P_0) the size of the droplets can be from a few nanometres to a few microns. As confirmed by spectroscopic studies of molecules isolated inside the droplets, the equilibrium temperature of the droplets is 0.37 ± 0.02 K and therefore, the droplets are superfluid.[1,6,34,35] Due to the superfluidity and weakly interacting nature of the droplets, molecules can vibrate and rotate almost freely inside the droplets. For most of the molecules, the ro-vibrational transitions in helium nanodroplets have been reported within 2 cm^{-1} of the transitions observed in the gas-phase studies.[1,6,36] However, the rotational constants for the molecules inside the droplets are found to be smaller than those for molecules in the gas phase. In general, the ratio of the rotational constants for the molecule in the gas phase (B_{gas}) and in helium droplets (B_{He}) increases as B_{gas} decreases. For example, the ratio for the HF molecule ($B_{gas} = 19.787\ cm^{-1}$ for ν_1 mode) is found to be 1.016,[37] whereas for $(CH_3)_3SiCCH$ molecule ($B_{gas} = 0.0654\ cm^{-1}$ for $2\nu_1$ mode), it is significantly larger, at 4.54.[38] This indicates a stronger coupling between molecular rotations and the surrounding helium for heavier molecules. The reduction in rotational constants in this superfluid medium, compared to a free molecule, arises because helium

This article is part of the Special Issue on 'Recent advances in physical chemistry research'.

Published online: 10 March 2026

atoms in the close vicinity of the molecule adiabatically follow the molecular rotation and thus contribute to the rotational constants.

Moreover, the superfluid helium droplets allow the formation of molecular clusters in a stepwise and sequential manner, which is crucial for studying different pathways of molecular aggregation and chemical reactions at the molecular level. At the cold temperatures, as provided by the helium droplets, it has been experimentally observed that the sequence in which molecules aggregate is crucial for the formation of a specific conformer of a molecular cluster or for a reaction to occur. For example, in helium droplets, aggregation of acetonitrile molecules in the presence of one HCl molecule resulted in the formation of exotic quasi-linear chains of $(\text{acetonitrile})_2$ – HCl along with the predominant formation of the global minimum structure, in which the acetonitrile-dimer unit is in an antiparallel arrangement.[39] However, when the aggregation sequence is reversed, i.e., when acetonitrile molecules aggregate first, followed by the addition of one HCl molecule, only the global minimum structure was observed with no formation of the chains. Similarly, the cyclic global minimum structure for the water tetramer has been invariably found in all the spectroscopic studies,[40–47] including those in helium nanodroplets.[5,48,49] However, it has been recently shown that an open-chain water tetramer moiety can also be formed in helium nanodroplets by aggregating water molecules in the presence of a single atom of neon.[50] Even the chemical reactivity at cold temperatures is found to be selective of the aggregation pathways. It has been observed that when the HCl molecule reacts with water molecules, the dissociation of HCl occurs on the addition of four water molecules to it. However, the dissociation is completely suppressed when the HCl molecule is added to a preformed water-tetramer or pentamer.[31]

Given the pivotal role of helium nanodroplets in enabling the investigation of molecular processes in a well-controlled manner, we have developed a helium nanodroplets isolation spectrometer in our laboratory at IIT Kanpur (HeNDI-IITK). In this article, we present the design of this newly fabricated spectrometer. As a proof-of-principle demonstration, we report the mass spectrum of helium nanodroplets and formic acid molecules isolated inside helium nanodroplets. We also report the detection method used for obtaining mass-selective infrared spectra of molecular species inside the droplets and demonstrate it with an example of the infrared spectrum of formic acid monomer.

2. Design and performance of the spectrometer

A photograph and schematic of the spectrometer are given in Figure 1. The design of the spectrometer closely follows that of other helium nanodroplets spectrometers used by research groups worldwide.[1,12,15,16,30,51–68] Our spectrometer comprises six differentially pumped vacuum chambers: (i) the expansion chamber, (ii), (iii) and (iv) three subsequent chambers, called pickup chambers (PC-I, PC-II and PC-III), (v) a buffer chamber and (vi) a detection chamber. All chambers were manufactured by Fourvac Technologies, Pune, India.

The expansion chamber (EC) is cylindrical, with a diameter of 400 mm and a height of 300 mm. This chamber houses a two-stage Gifford-McMahon Cryocooler (SHI-CH210, minimum temperature 10 K) that has a first-stage cooling power of 110 W at 77 K and a second-stage cooling power of 6 W at 20 K, with a 50 Hz power supply. The cryocooler is customised to cool down a nozzle plate with a 5-micron orifice to the desired temperature range of, typically, 10–20 K, details of which are in the next paragraph. The cryocooler operates in conjunction with a water-cooled closed-cycle helium compressor (SHI, F-70). It is connected to the expansion chamber through an X–Y translational stage, which facilitates its movement in a plane by ± 5 mm in both perpendicular directions. The expansion chamber is pumped by an oil diffusion pump (Leybold DIP8000, pumping speed 8000 L/s for air), which is backed by a rotary vane pump (Leybold Trivac-D 65B, pumping speed 65 m^3/h for air) and a booster pump (Leybold RUVAC-WAU-251, pumping speed 210 m^3/h for air). The minimum pressure achieved in this chamber without a helium gas load is $\sim 2 \times 10^{-7}$ mbar.

A rendering of the customised cryostat from its 3D-CAD model is shown in Figure 2. The helium gas flows from room temperature through a 1/4" stainless-steel tube and is guided inside the expansion chamber via a gas port on the vacuum shroud of the cryostat. Just before the gas port, an in-line 2-μ sintered filter is installed to block any microparticles entering the gas line, which might clog the nozzle orifice. This stainless-steel tube is welded to a 1/16" copper tube. Approximately 272 cm (8 rounds) of this copper tube is coiled around the first stage of cooling, and $\sim$278 cm (13 rounds) is coiled around the second stage of cooling to increase the surface contact with the cryostat. At the second stage, the helium gas cools down to a minimum temperature of $\sim$10 K. The gas then enters a copper reservoir, which is coupled to the second stage of cooling through an extension rod

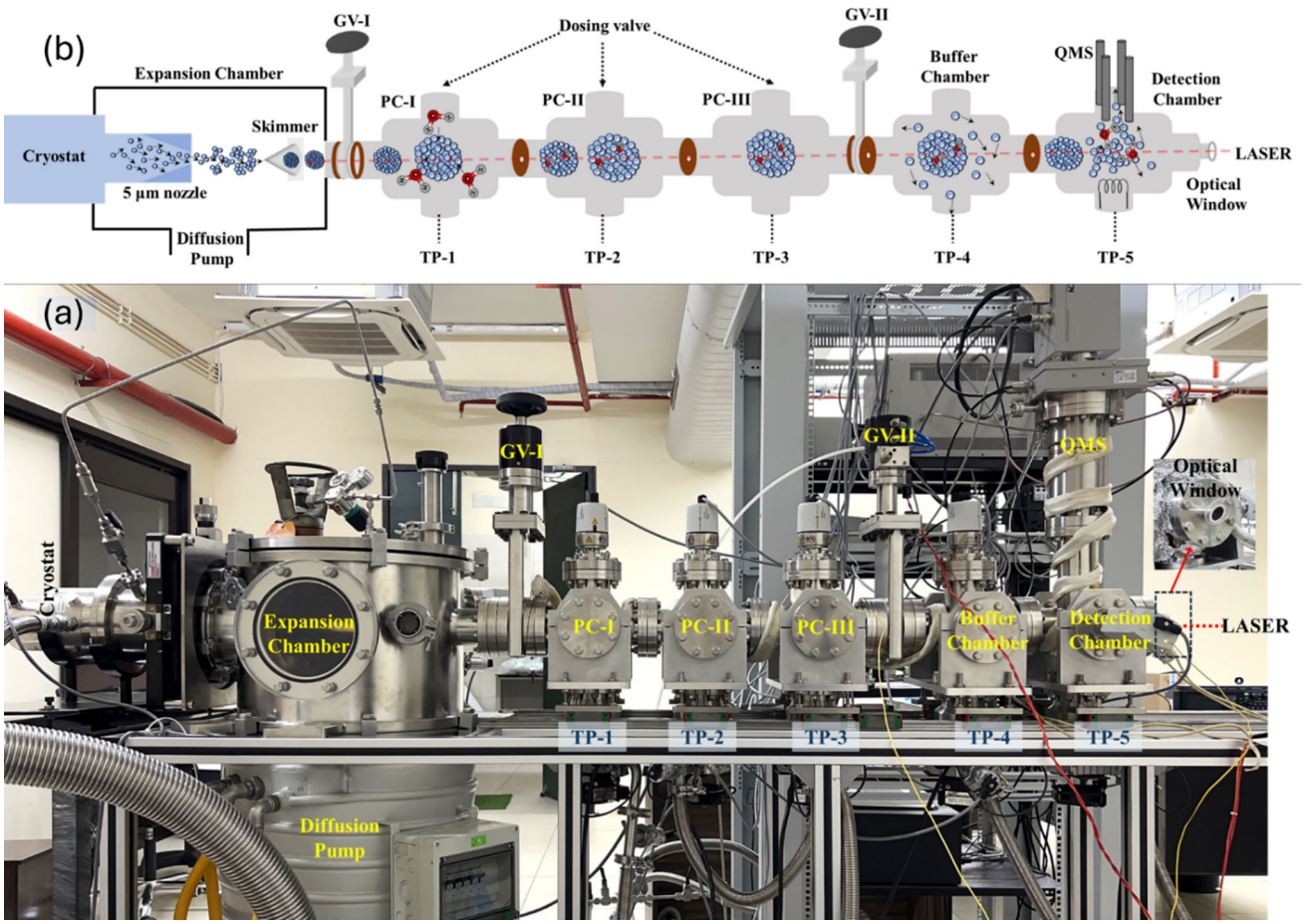

Figure 1. (**a**) Photograph and (**b**) the schematics of the helium nanodroplets isolation spectrometer at IIT Kanpur (HeNDI-IITK). TP: Turbomolecular pump; PC: Pickup chamber; GV: Gate valve; QMS: Quadrupole mass spectrometer.

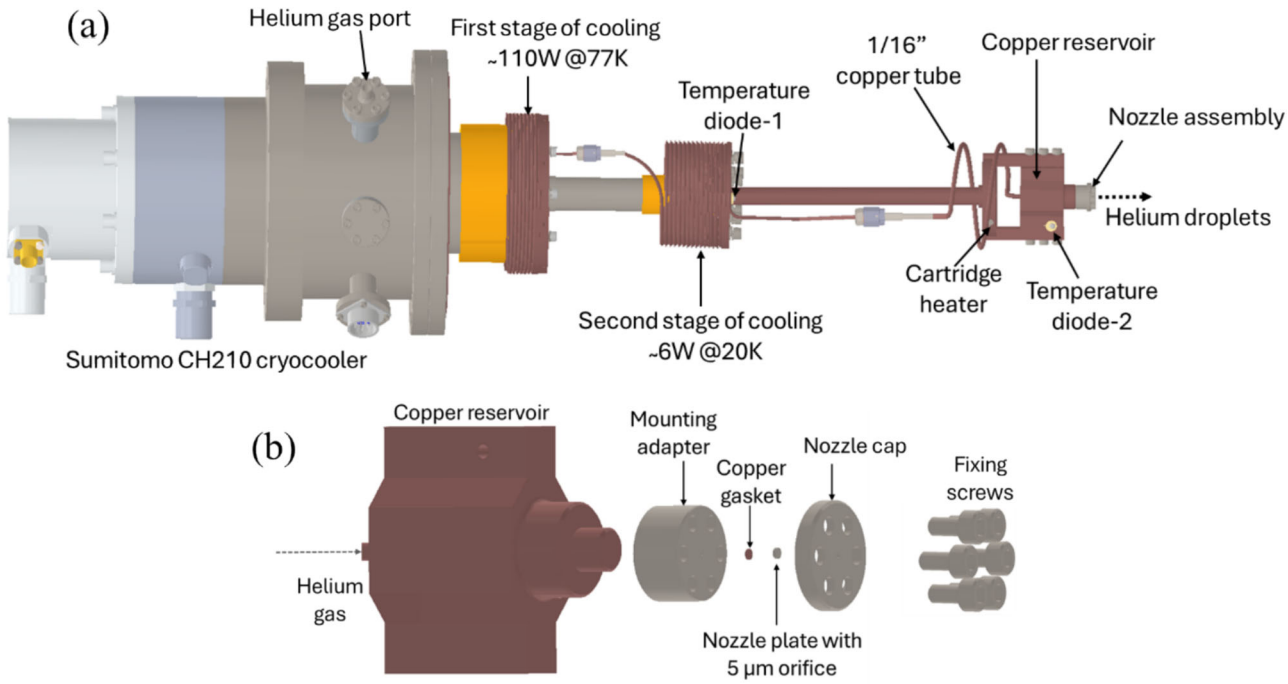

Figure 2. (**a**) Customised cryostat with nozzle assembly and (**b**) expanded view of the nozzle assembly.

(24.6 cm) made of OFHC copper. On the other end of the reservoir, the 5-micron nozzle plate is connected (Figure 2(a) and (b)). The length of the copper extension rod was chosen to keep the distance between the nozzle and the skimmer orifice to ~1.5 cm. The 5 μm platinum nozzle (95/5% Platinum-Iridium alloy, 2 mm diameter and 0.6 mm thickness, Plano-AGA0200P) is sealed to the copper reservoir using an OFHC copper gasket (2 mm diameter and 0.4 mm thickness). Temperatures are monitored at two different points, Figure 2(a), one near the second stage of the cryostat and the other at the reservoir, using two silicon diode sensors (Lakeshore, DT-670). A 50-watt cartridge heater in conjunction with a temperature controller (Lakeshore Model 335) is used to vary and maintain the temperature of the nozzle assembly.

In between the expansion chamber and the first pickup chamber, a conical skimmer of 0.5 mm orifice (nickel, Beamdynamics model 2) is placed to collimate the helium nanodroplets beams generated in the expansion chamber. A manual gate valve is placed between the skimmer and the PC-I. This valve allows us to vent the expansion chamber whenever required without breaking the vacuum of the rest of the chambers. The three pickup chambers are interconnected via customised conflat copper discs with a 5 mm orifice at their centre. These discs help in achieving differential pumping and in minimising the effusion of sample molecules from one chamber to the other. All the pickup chambers and the buffer chamber are standard CF-63 six-way crosses with symmetrical dimensions of 210 mm in the three perpendicular directions. For the detection chamber, one of the lengths is increased to 280 mm to host a Quadrupole Mass Spectrometer (QMS, Hiden Analytics, HAL/3F-RC-PIC), which has a crossbeam ionisation source with an orifice of 4 mm. The helium nanodroplets beams generated in the expansion chambers pass through the 0.5 mm skimmer, then the 5 mm orifices of the copper discs in between the chambers, and finally, the 4 mm aperture of the QMS, where electron ionisation occurs. Each of the five chambers is pumped by dedicated turbomolecular pumps (Edwards nEXT 85D, pumping speed 84 L/s for nitrogen) backed by rotary vane pumps. Pressures for the expansion, PC-I, PC-II, PC-III, and buffer chambers are monitored using dedicated cold cathode vacuum gauges (Pfeiffer IKR 251, range 1×10^{-2} to 2×10^{-9} mbar), and that of the QMS chamber is measured using a full-range Bayard–Alpert gauge (Pfeiffer PBR 260, range 1000 to 5×10^{-10} mbar). The three pickup chambers are also equipped with dosing valves (VAT series 59.0, DN16, all-metal variable leak valve), which are used to introduce vapours of the molecules of interest into these chambers. The minimum pressure achieved in all the chambers at ~300 K without gas load are given in Table 1. Since the helium droplets are sensitive to background gases (N_2, O_2, H_2O, etc.) and readily pickup any atom/molecule on their path, it is a must to maintain a high vacuum throughout their path. For this, we periodically bake out these chambers at ~100°C.

3. Generation and detection of the helium nanodroplets

In our lab, we generally form helium nanodroplets using initial conditions T_0 = 10–20 K and P_0 = 15–50 bar. When the helium droplets are generated, and the alignment of the nozzle is such that the droplets reach the detection chamber, a noticeable increase in pressure in all the chambers is observed. The pressures observed in the chambers for 11 K nozzle temperature and different helium pressures are given in Table 1.

After travelling through all the chambers, the droplets pass through the 4 mm orifice of the crossbeam ionisation source of the QMS. Here, the droplets are ionised via electron ionisation (typically, 70–100 eV). The additional energy imparted into the droplets as a result of interaction with the high-energy electrons leads to their fragmentation, and He_n^+ clusters are formed. The ionised fragments then pass through a quadrupole filter and are eventually detected by a secondary electron multiplier.

We generated the droplets under the initial source conditions of $T_0 = 11$ K and $P_0 = 20$ bar. The mass spectrum of these droplets, recorded with 80 eV electron energy over the range of m/z = 6–400 u, is shown in Figure 3. For the range of m/z = 6–100 u, a filament current of 200 μA and for m/z = 100–400 u, a filament current of 400 μA was used to improve the signal intensity. The spectrum shows characteristic peaks at multiples of $m/z = 4$, which correspond to the He_n^+ fragments. In general, the intensities of the fragments decrease monotonically with increasing m/z, with a few exceptions, such as fragments at 28, 32, 40, 44, 52 and 56, which have more intensities than expected. This is well known in the community and is mainly attributed to the higher stability of the corresponding He_n^+ clusters.[29] Intensity observed at $m/z = 28$ also has a minor contribution from $N_2^{\bullet+}$ fragment originating from residual nitrogen in the apparatus.

Table 1. Pressures (in mbar) for different chambers at different initial conditions.

	Expansion chamber	PC-I	PC-II	PC-III	Buffer chamber	Detection chamber
~300 K, without helium (GV-I and GV-II Closed)	$\sim 2 \times 10^{-7}$	$< 2 \times 10^{-9}$	$< 2 \times 10^{-9}$	$< 2 \times 10^{-9}$	$< 2 \times 10^{-9}$	$\sim 5 \times 10^{-10}$
With helium gas load (GV-I and GV-II open)						
$T_0 = 11\,\text{K}, P_0 = 20\,\text{bar}$	5.5×10^{-5}	2.2×10^{-6}	1.4×10^{-7}	2.1×10^{-8}	1.9×10^{-8}	3.3×10^{-9}
$T_0 = 11\,\text{K}, P_0 = 30\,\text{bar}$	6.8×10^{-5}	3.5×10^{-6}	2.3×10^{-7}	2.6×10^{-8}	2.4×10^{-8}	6.3×10^{-9}
$T_0 = 11\,\text{K}, P_0 = 40\,\text{bar}$	8.8×10^{-5}	4.8×10^{-6}	3.4×10^{-7}	3.1×10^{-8}	2.9×10^{-8}	1.2×10^{-8}

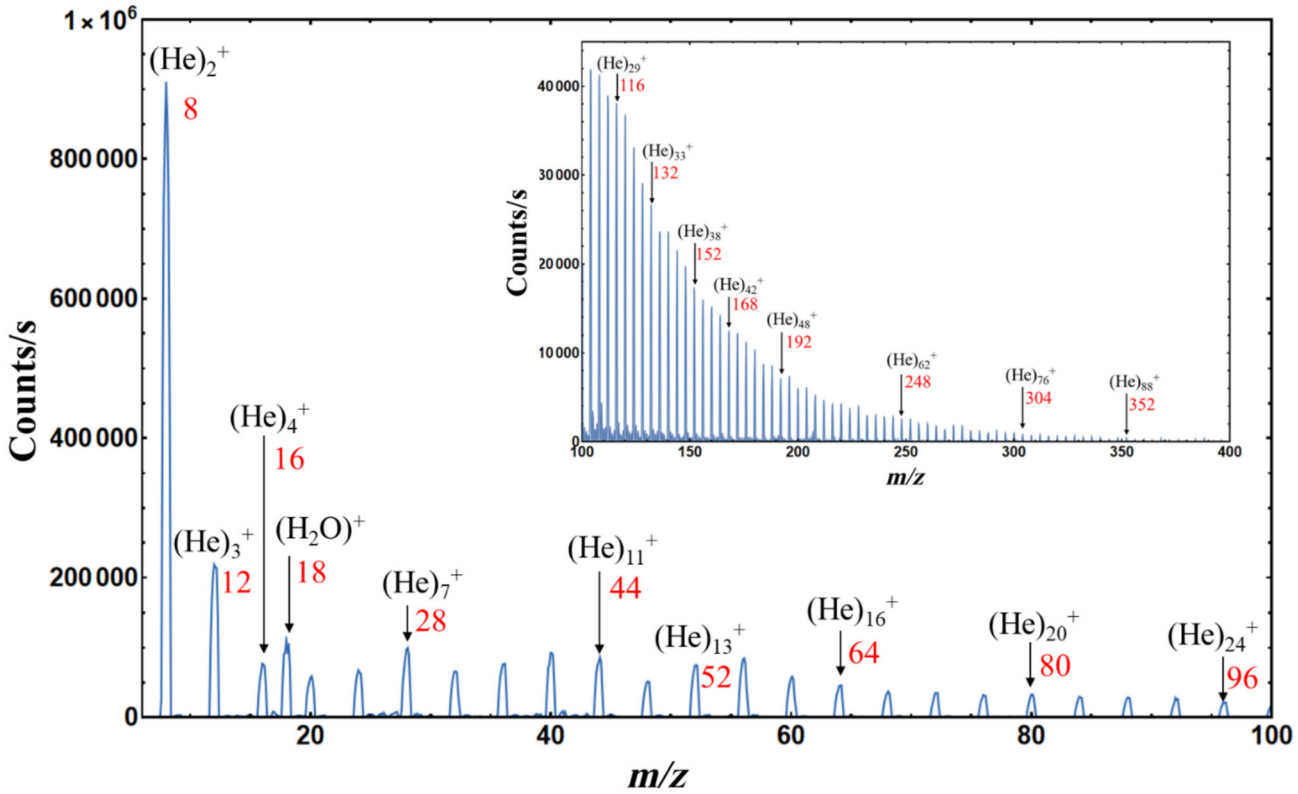

Figure 3. Mass spectrum of helium nanodroplets, generated at $T_0 = 11\,\text{K}, P_0 = 20\,\text{bar}$, over the range of 6–100 u (80 eV electron energy, 200 μA filament current) and 100–400 u (80 eV electron energy, 400 μA filament current). Peak at m/z = 18 originates from residual water in the apparatus.

4. Isolation of the molecules inside the helium nanodroplets

The molecules of interest can be introduced into any or all three pickup chambers. As the droplets pass through these chambers, they capture the molecules, enabling the isolation of single molecules and the formation of molecular aggregates. The pickup of the molecules by the droplets follows Poisson statistics, and the average number of molecules captured by the droplets can be controlled by adjusting the partial pressures of the dopants in the pickup chambers. The use of three separate pickup chambers provides independent control over the partial pressures of up to three different dopant species, allowing formation of molecular aggregates in different size ratios with excellent control.

In this work, we isolated formic acid molecules in the droplets. For this, vapours of formic acid (99%, Sigma Aldrich) were introduced in the first pickup chamber at a partial pressure of 2.5×10^{-6} mbar. The

resulting mass spectrum of the droplets embedded with formic acid molecules is shown in Figure 4. The observed low-intensity peak at $m/z = 46$, corresponds to the $HCOOH^{\bullet+}$ fragment. The most prominent peak is observed at $m/z = 29$, which corresponds to the CHO^+ fragment formed by the loss of a hydroxy radical from $HCOOH^{\bullet+}$. The peak observed at $m/z = 45$ corresponds to $HCOO^+$ fragments, which are formed by the loss of a hydrogen atom from $HCOOH^{\bullet+}$, while the peaks observed at $m/z = 28$ and 44 correspond to CO^+(and He_7^+) and CO_2^+(and He_{11}^+) fragments, respectively. Peaks observed at $m/z = 19, 47, 91, 92$ and 93 correspond to H_3O^+, $(HCOOH)H^+$, $(HCOOH)HCOO^+$, $(HCOOH)_2^{\bullet+}$ and $(HCOOH)_2H^+$ fragments, respectively. These fragments arise from oligomers of formic acid, such as dimers and trimers.

5. Mass-selective infrared spectroscopy of molecular species isolated inside helium nanodroplets

To record mass-selective infrared spectra of molecular species isolated in the helium droplets, we have coupled our machine with a tunable high-resolution mid-IR laser source (Toptica Photonics TOPO), Figure 5. The laser source is a continuous wave optical parametric oscillator, which is pumped by a Distributed-Feedback-Diode laser (DFB-Pro-BFY, 1064 nm, tunability of ~700 GHz). The output of the pump laser is power amplified to 10 watts using a Fibre amplifier (IPG photonics, YAR-10-1064-LP-SF). This pump beam is split into a signal (1.45–2.07 μm, 4830–6900 cm^{-1}) and an idler beam (2.19–4.00 μm, 2500–4570 cm^{-1}) by passing it through a non-linear crystal. The idler radiation is tunable with a frequency resolution as good as 0.0001 cm^{-1}. The wavelength of the pump and signal beam is monitored using a wavelength meter (Highfiness WS/6-200, measurement range 0.5–2.25 μm, accuracy 200 MHz), from which the wavelength of the idler beam is calculated using $1/\lambda_{idler} = 1/\lambda_{pump} - 1/\lambda_{signal}$.

Helium droplets are transparent to IR radiation. However, when exposed to mid-infrared radiation resonant with the molecular transitions, the embedded molecules become vibrationally excited. The molecules then relax back to their ground state by transferring the excess energy to the surrounding helium droplets. This leads to the evaporation of several hundred helium atoms (approximately one helium atom per 5 cm^{-1} energy) from the droplets, resulting

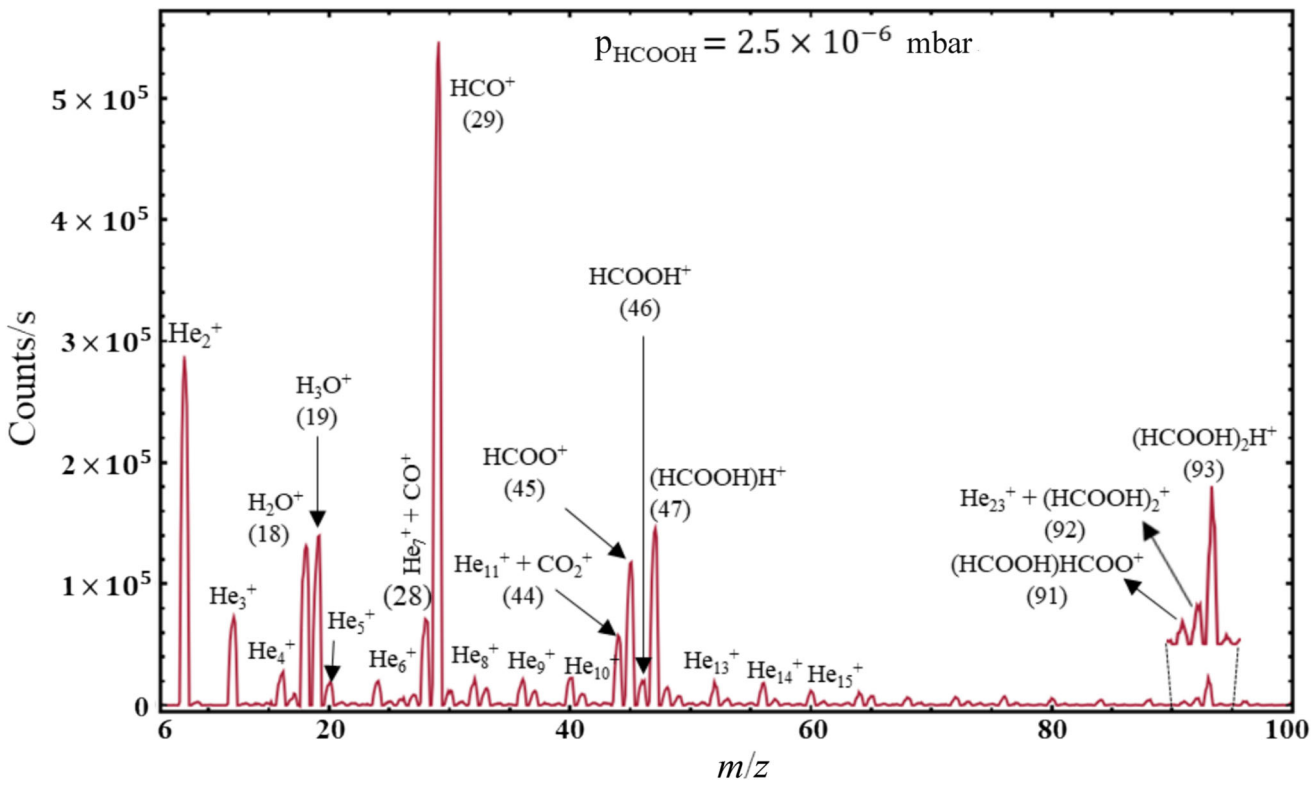

Figure 4. Mass spectrum of helium nanodroplets ($T_0 = 11$ K, $P_0 = 20$ bar) embedded with formic acid molecules at a formic acid partial pressure of 2.5×10^{-6} mbar. The spectrum was recorded with 80 eV electron energy and 100 μA filament current.

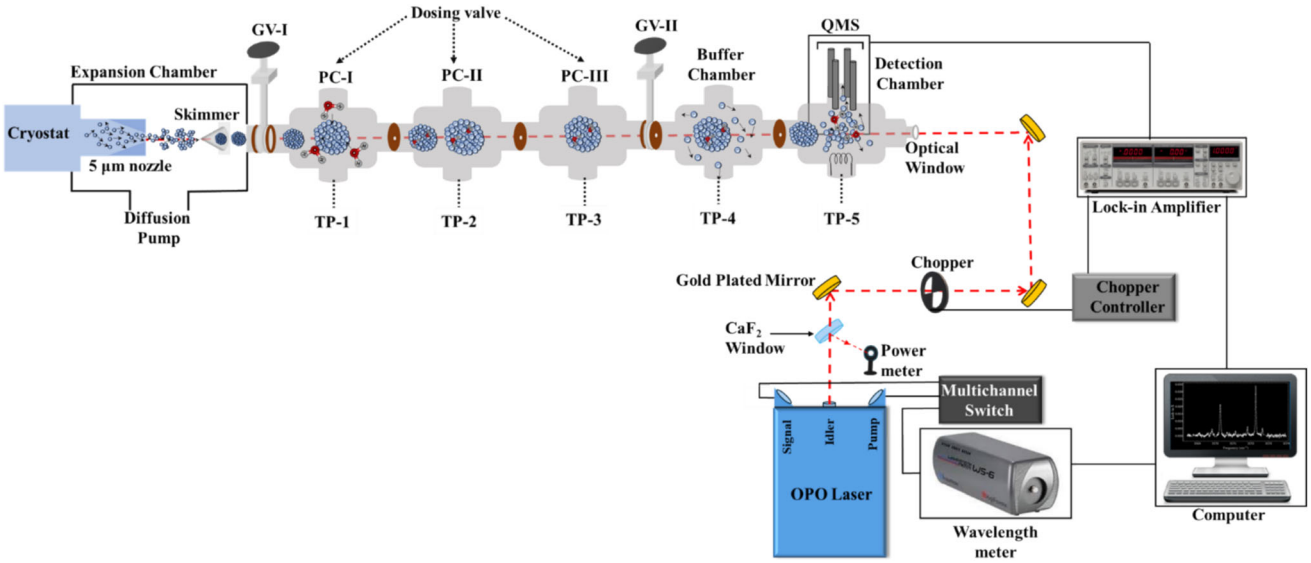

Figure 5. Schematics of the helium nanodroplets isolation spectrometer coupled with a mid-infrared laser radiation source.

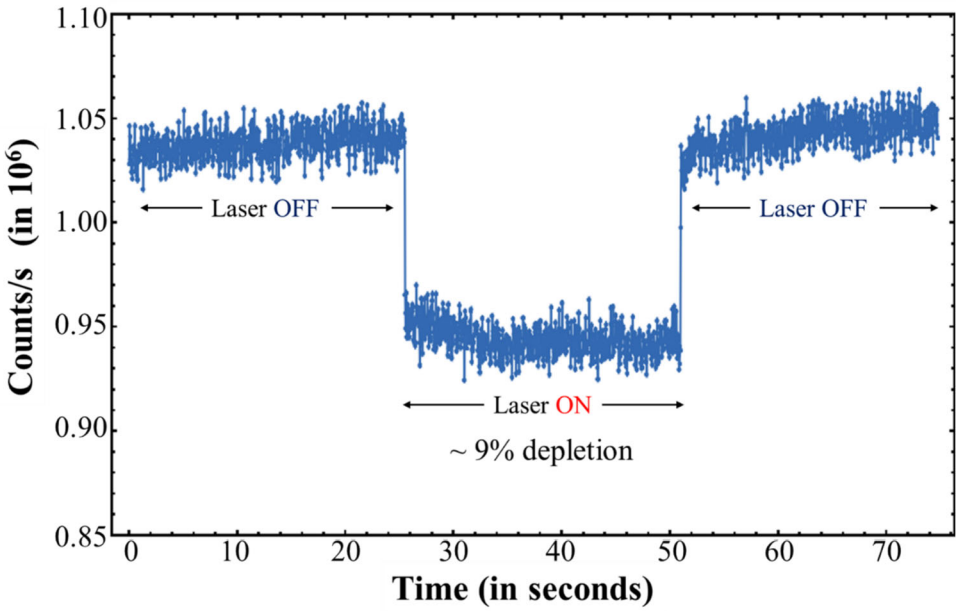

Figure 6. Effect of laser radiation of frequency 3572.2940 cm^{-1} on the ion current for m/z = 29 (CHO^+ fragment).

in a reduced electron ionisation cross-section of the droplets. Consequently, on resonance, the laser radiation produces a dip in the ion currents of fragments. This depletion is detected via phase-sensitive detection with a lock-in amplifier (SRS, SR-850). An optical chopper, which modulates the laser at a frequency of 10 Hz, is used as a reference for the lock-in amplifier. Recording the depletion in the ion current as a function of laser frequency yields the infrared spectrum of the embedded molecule.

We once again selected formic acid as a model system to test the performance of our spectrometer. The formic acid monomer has been studied previously in helium nanodroplets.[69–72] Madeja *et al.*[69] reported well-resolved ro-vibrational features in the O–H and C–H stretching ranges. However, the study was non-mass selective since a bolometer was used as a detector. More recently, Meyer *et al.*[70] reported mass-selective infrared spectra of formic acid in helium nanodroplets and reported the O–H vibrational band

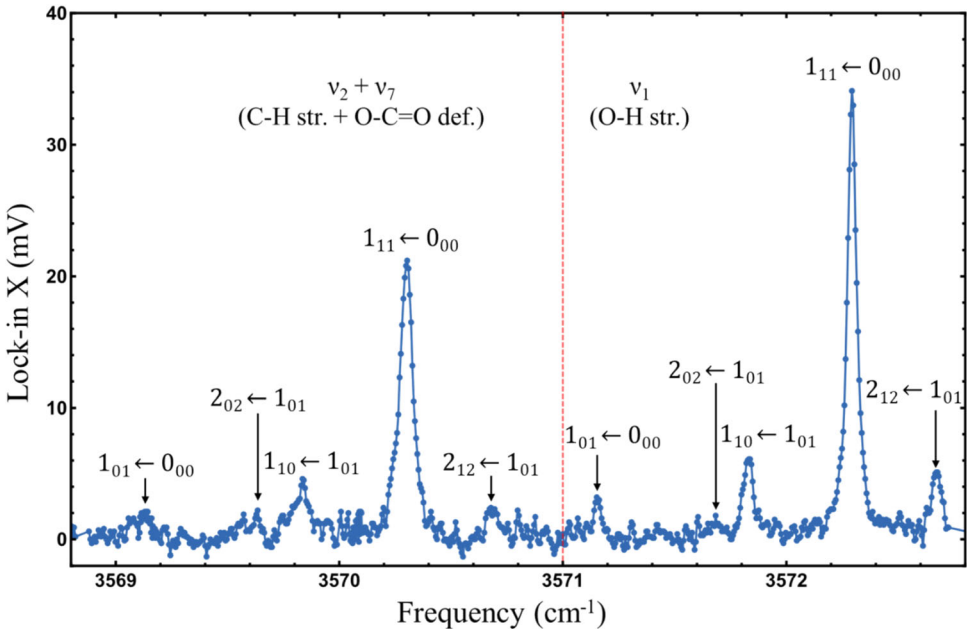

Figure 7. Mass-selective infrared spectrum of formic acid embedded in helium nanodroplets, measured at m/z = 29 u. The dotted line separates the transitions of the O–H stretching band from those of the C–H stretching + O–C=O deformation combination band. The assignments are adapted from Madeja *et al.*[69]

for the monomer at $\sim$3570 cm^{-1}. However, due to the use of a pulsed laser source with a bandwidth of 4 cm^{-1}, the rotational information was absent.

In our measurements, we first fixed the laser frequency at 3572.2940 cm^{-1}, which corresponds to the $v = 1(1_{11}) \leftarrow v = 0(0_{00})$ ro-vibrational transition of the OH stretching band of formic acid monomer. The laser power was set to $\sim$800 mW. The ion current of the CHO^+ fragment ($m/z = 29$) of formic acid was recorded when the laser was blocked (off) and unblocked (on). As shown in Figure 6, exposure of the doped droplets to laser radiation resulted in $\sim$9% depletion of the $m/z = 29$ ion current, indicating a significant reduction in the ionisation cross-section of the droplets due to ro-vibrational excitation of the embedded formic acid molecules.

The infrared spectrum was then recorded by scanning the laser frequency and monitoring the ion current at $m/z = 29$ with the lock-in amplifier such that a positive lock-in signal corresponds to depletion in the ion current. The resulting mass-selective spectrum in the range of $\sim$3568.8–3572.7 cm^{-1}, obtained at $\sim$0.005 cm^{-1} resolution, is shown in Figure 7.

A total of ten well-resolved ro-vibrational transitions, corresponding to the O–H stretching and C–H stretching + O–C=O deformation combination bands of the formic acid monomer, were observed. The rotational assignments $(J'_{K'_aK'_c} \leftarrow J''_{K''_aK''_c})$ of the observed transitions are indicated in Figure 7. These assignments are based on the previous assignments by Madeja *et al.*[69] The spectrum presented in Figure 7 is in excellent agreement with that reported previously by Madeja *et al.*[69] confirming the performance of our spectrometer.

6. Conclusion and outlook

We have presented the design and implementation of a newly developed helium nanodroplets isolation spectrometer at IIT Kanpur. Its operation was demonstrated through the mass spectra of pure helium nanodroplets and helium nanodroplets doped with formic acid molecules. Furthermore, we reported the mass-selective infrared spectrum of the formic acid monomer in the range $\sim$3568.8–3572.7 cm^{-1}.

Currently, the spectrometer enables the investigation of molecules that can be isolated into droplets from samples with sufficient vapour pressure. In the future, we plan to integrate a vacuum oven to allow studies of low-volatility compounds that can be vaporised through heating. This will enable the isolation and further analysis of, for example, small biomolecules in the droplets. We also plan to add a pyrolysis source for studying molecular radicals. This will also facilitate studies of reactions of these radicals with neutral molecules.

Acknowledgements

The authors gratefully acknowledge the support from IIT Kanpur through the Initiation Grant (IITK/CHM/2020118) and Special Research Grants (R&D/CHM/2021208 and R&D/CHM/2023019), as well as from ANRF-India (formerly SERB-India) under the Core Research Grant (CRG/2022/001181), which together provided major funding for the spectrometer. Additional support from BRNS-India (58/14/10/2023-BRNS/11696) and ISRO-India (STC-IITK Cell, STC/CHM/2023664F) is also sincerely appreciated. The authors also thank Dr. Manish K. Tripathi and Dr. Surendra V. Singh for their assistance during the initial phase of setting up the spectrometer. RG acknowledges UGC-India for a research fellowship, while SS, Yashika, PR and PK acknowledge IIT Kanpur for research fellowships.

References

1. Hartmann M, Miller R E, Toennies J P and Vilesov A F 1995 Rotationally resolved spectroscopy of SF_6 in liquid helium clusters: A molecular probe of cluster temperature *Phys. Rev. Lett.* **75** 1566
2. Toennies J P and Vilesov A F 1998 Spectroscopy of atoms and molecules in liquid helium *Annu. Rev. Phys. Chem.* **49** 1
3. Hartmann M, Pörtner N, Sartakov B, Toennies J P and Vilesov A F 1999 High resolution infrared spectroscopy of single SF_6 molecules in helium droplets I. Size effects in ^{4}He droplets. *J. Chem. Phys.* **110** 5109
4. Nauta A K and Miller R E 1999 Nonequilibrium self-assembly of long chains of polar molecules in superfluid helium *Science* **283** 1895
5. Nauta K and Miller R E 2000 Formation of cyclic water hexamer in liquid helium: The smallest piece of ice *Science* **287** 293
6. Grebenev S, Hartmann M, Havenith M, Sartakov B, Toennies J P and Vilesov A F 2000 The rotational spectrum of single OCS molecules in liquid ^{4}He droplets *J. Chem. Phys.* **112** 4485
7. Nauta K and Miller R E 2001 The vibrational and rotational dynamics of acetylene solvated in superfluid helium nanodroplets *J. Chem. Phys.* **115** 8384
8. Nauta K and Miller R E 2001 Rotational and vibrational dynamics of methane in helium nanodroplets *Chem. Phys. Lett.* **350** 225
9. Douberly G E and Miller R E 2003 The growth of HF polymers in helium nanodroplets: probing the barriers to ring insertion *J. Phys. Chem. B* **107** 4500
10. Toennies J P and Vilesov A F 2004 Superfluid helium droplets: A uniquely cold nanomatrix for molecules and molecular complexes *Angew. Chem., Int. Ed.* **43** 2622
11. Merritt J M, Küpper J and Miller R E 2005 Entrance channel X-HF (X = Cl, Br and I) complexes studied by high-resolution infrared laser spectroscopy in helium nanodroplets *Phys. Chem. Chem. Phys.* **7** 67
12. von Haeften K, Rudolph S, Simanovski I, Havenith M, Zillich R E and Whaley K B 2006 Probing phonon–rotation coupling in helium nanodroplets: Infrared spectroscopy of CO and its isotopomers *Phys. Rev. B* **73** 054502
13. Lindsay C M, Douberly G E and Miller R E 2006 Rotational and vibrational dynamics of H_2O and HDO in helium nanodroplets *J. Mol. Struct.* **786** 96
14. Choi M Y and Miller R E 2006 Four tautomers of isolated guanine from infrared laser spectroscopy in helium nanodroplets *J. Am. Chem. Soc.* **128** 7320
15. Lehnig R and Jäger W 2006 Infrared spectroscopy of the antisymmetric stretching mode of $^{16}OC^{18}O$ in helium nanodroplets *Chem. Phys. Lett.* **424** 146
16. Choi M Y, Douberly G E, Falconer T M, Lewis W K, Lindsay C M, Merritt J M, Stiles P L and Miller R E 2006 Infrared spectroscopy of helium nanodroplets: novel methods for physics and chemistry *Int. Rev. Phys. Chem.* **25** 15
17. Skvortsov D, Choi M Y and Vilesov A F 2007 Study of HCl clusters in helium nanodroplets: experiments and *ab initio* calculations as stepping stones from gas phase to bulk *J. Phys. Chem. A* **111** 12711
18. Gutberlet A, Schwaab G, Birer Ö, Masia M, Kaczmarek A, Forbert H, Havenith M and Marx D 2009 Aggregation-induced dissociation of $HCl(H_2O)_4$ below 1 K: The smallest droplet of acid *Science* **324** 1545
19. Krasnokutski S A and Huisken F 2010 Oxidative reactions of silicon atoms and clusters at ultralow temperature in helium droplets *J. Phys. Chem. A* **114** 13045
20. Morrison A M, Flynn S D, Liang T and Douberly G E 2010 Infrared spectroscopy of $(HCl)_m(H_2O)_n$ clusters in helium nanodroplets: definitive assignments in the HCl stretch region *J. Phys. Chem. A* **114** 8090
21. Gomez L F, Loginov E, Sliter R and Vilesov A F 2011 Sizes of large He droplets *J. Chem. Phys.* **135** 154201
22. Morrison A M, Agarwal J, Schaefer H F III and Douberly G E 2012 Infrared laser spectroscopy of the CH_3OO radical formed from the reaction of CH_3 and O_2 within a helium nanodroplet *J. Phys. Chem. A* **116** 5299
23. Moradi C P, Morrison A M, Klippenstein S J, Goldsmith C F and Douberly G E 2013 Propargyl + O_2 reaction in helium droplets: entrance channel barrier or not? *J. Phys. Chem. A* **117** 13626
24. Yang S and Ellis A M 2013 Helium droplets: A chemistry perspective *Chem. Soc. Rev.* **42** 472
25. Raston P L, Douberly G E and Jäger W 2014 Single and double resonance spectroscopy of methanol embedded in superfluid helium nanodroplets *J. Chem. Phys.* **141** 044301
26. Krasnokutski S A and Huisken F 2014 Ultra-low-temperature reactions of $C(^3P_0)$ atoms with benzene molecules in helium droplets *J. Chem. Phys.* **141** 07292
27. Sliter R, Gomez L F, Kwok J and Vilesov A F 2014 Sizes distributions of large He droplets *Chem. Phys. Lett.* **600** 29
28. Sulaiman M I, Yang S and Ellis A M 2017 Infrared spectroscopy of methanol and methanol/water clusters in helium nanodroplets: The OH stretching region *J. Phys. Chem. A* **121** 771
29. Mauracher A, Echt O, Ellis A M, Yang S, Bohme D K, Postler J, Kaiser A, Denifl S and Scheier P 2018 Cold physics and chemistry: collisions, ionization and

reactions inside helium nanodroplets close to zero K *Phys. Rep.* **751** 1
30. Verma D, Tanyag R M P, O'Connell S M O and Vilesov A F 2019 Infrared spectroscopy in superfluid helium droplets *Adv. Phys. X* **4** 1553569
31. Mani D, De Tudela R P, Schwan R, Pal N, Körning S, Forbert H, Redlich B, van der Meer A F G, Schwaab G, Marx D and Havenith M 2019 Acid solvation versus dissociation at "stardust conditions": reaction sequence matters *Sci. Adv.* **5** eaav8179
32. Toennies J P 2022 In *Molecules in Superfluid Helium Nanodroplets: Spectroscopy, Structure, and Dynamics* (*Topics in Applied Physics* - vol. 145) Slenczka A and Toennies J P (eds.) (Springer Nature: Switzerland) p. 1
33. Jäger S, Khatri J, Meyer P, Henkel S, Schwaab G, Nandi A, Pandey P, Barlow K R, Perkins M A, Tschumper G S, Bowman J M, van der Avoird A and Havenith M 2024 On the nature of hydrogen bonding in the H_2S dimer *Nat. Commun.* **15** 1
34. Grebenev S, Toennies J P and Vilesov A F 1998 Superfluidity within a small helium-4 cluster: The microscopic Andronikashvili experiment *Science* **279** 2083
35. Grebenev S, Sartakov B, Toennies J P and Vilesov A F 2000 Evidence for superfluidity in Para-Hydrogen clusters inside helium-4 droplets at 0.15 K *Science* **289** 1532
36. Behrens M, Buck U, Fröchtenicht R, Hartmann M, Huisken F and Rohmund F 1998 Rotationally resolved IR spectroscopy of ammonia trapped in cold helium clusters *J. Chem. Phys.* **109** 5914
37. Nauta K and Miller R E 2000 Metastable vibrationally excited HF ($v = 1$) in helium nanodroplets *J. Chem. Phys.* **113** 9466
38. Callegari C, Conjusteau A, Reinhard I, Lehmann K K and Scoles G 2000 First overtone helium nanodroplet isolation spectroscopy of molecules bearing the acetylenic CH chromophore *J. Chem. Phys.* **113** 10535
39. Mani D, Roy T K, Khatri J, Schwaab G, Blach S, Hölzl C, Forbert H, Marx D and Havenith M 2022 Internal electric field-induced formation of exotic linear acetonitrile chains *J. Phys. Chem. Lett.* **13** 6852
40. Cruzan J D, Braly L B, Liu K, Brown M G, Loeser J G and Saykally R J 1996 Quantifying hydrogen bond cooperativity in water: VRT spectroscopy of the water tetramer *Science* **271** 59
41. Huisken F, Kaloudis M and Kulcke A 1996 Infrared spectroscopy of small size-selected water clusters *J. Chem. Phys.* **104** 17
42. Cruzan J D, Viant M R, Brown M G and Saykally R J 1997 Terahertz laser vibration–rotation tunneling spectroscopy of the water tetramer *J. Phys. Chem. A* **101** 9022
43. Paul J B 1999 Infrared cavity Ringdown spectroscopy of the water cluster bending vibrations *J. Phys. Chem. A* **103** 2972
44. Keutsch F N and Saykally R J 2001 Water clusters: untangling the mysteries of the liquid, one molecule at a time *Proc. Natl. Acad. Sci. USA* **98** 10533
45. Hirabayashi S and Yamada K M T 2005 Infrared spectra of water clusters in krypton and xenon matrices *J. Chem. Phys.* **122** 244501
46. Ceponkus J, Uvdal P and Nelander B 2012 Water tetramer, pentamer, and hexamer in inert matrices *J. Phys. Chem. A* **116** 4842
47. Zhang B, Yu Y, Zhang Y Y, Jiang S, Li Q, Hu H-S, Li G, Zhao Z, Wang C, Xie H, Zhang W, Dai D, Wu G, Zhang D H, Jiang L, Li J and Yang X 2020 Infrared Spectroscopy of neutral water clusters at finite temperature: evidence for a noncyclic pentamer *Proc. Natl. Acad. Sci. USA* **117** 15423–15428
48. Slipchenko M N, Kuyanov K E, Sartakov B G and Vilesov A F 2006 Infrared intensity in small ammonia and water clusters *J. Chem. Phys.* **124** 211101
49. Schwan R, Kaufmann M, Leicht D, Schwaab G and Havenith M 2016 Infrared spectroscopy of the ν_2 band of the water monomer and small water clusters $(H_2O)_{n=2,3,4}$ in helium droplets *Phys. Chem. Chem. Phys.* **18** 24063
50. Douberly G E, Miller R E and Xantheas S S 2017 Formation of exotic networks of water clusters in helium droplets facilitated by the presence of neon atoms *J. Am. Chem. Soc.* **139** 4152
51. Callicoatt B E, Förde K, Ruchti T, Jung L, Janda K C and Halberstadt N 1998 Capture and ionization of argon within liquid helium droplets *J. Chem. Phys.* **108** 9371
52. Slipchenko M N, Kuma S, Momose T and Vilesov A F 2002 Intense pulsed helium droplet beams *Rev. Sci. Instrum.* **73** 3600
53. Yang S, Brereton S M, Wheeler M D and Ellis A M 2005 Soft or hard ionization of molecules in helium nanodroplets? An electron impact investigation of alcohols and ethers *Phys. Chem. Chem. Phys.* **7** 4082
54. Peterka D S, Kim J H, Wang C C, Poisson L and Neumark D M 2007 Photoionization dynamics in pure helium droplets *J. Phys. Chem. A* **111** 7449
55. Pentlehner D, Riechers R, Dick B, Slenczka A, Even U, Lavie N, Brown R and Luria K 2009 Rapidly pulsed helium droplet source *Rev. Sci. Instrum.* **80** 043302
56. Ravi A, Kuma S, Yearwood C, Kahlon B, Mustafa M, Al-Basheer W, Enomoto K and Momose T 2011 ν_4 Band of CH_4 in helium nanodroplets: A probe of the dynamical response of a superfluid *Phys. Rev. A* **84** 020502
57. An der Lan L, Bartl P, Leidlmair C, Schöbel H, Jochum R, Denifl S, Märk T D, Ellis A M and Scheier P 2011 The submersion of sodium clusters in helium nanodroplets: Identification of the surface → interior transition *J. Chem. Phys.* **135** 044309
58. Loginov E, Gomez L F and Vilesov A F 2011 Surface deposition and imaging of large Ag clusters formed in He droplets *J. Phys. Chem. A* **115** 7199
59. Cleaver R M and Lindsay C M 2012 Detailed design and transport properties of a helium droplet nozzle from 5 to 50 K *Cryogenics* **52** 389
60. Hernando A, Masson A, Briant M, Mestdagh J M, Gaveau M A and Halberstadt N 2012 Fluorescence emission of Ca-atom from photodissociated Ca_2 in Ar doped helium droplets. II Theoretical *J. Chem. Phys.* **137** 184311
61. Morrison A M, Liang T and Douberly G E 2013 Automation of an "Aculight" continuous-wave optical parametric oscillator *Rev. Sci. Instrum.* **84** 013102

62. Buchta D, Krishnan S R, Brauer N B, Drabbels M, O'Keeffe P, Devetta M, Di Fraia M, Callegari C, Richter R, Coreno M, Prince K C, Stienkemeier F, Moshammer R and Mudrich M 2013 Charge transfer and Penning ionization of dopants in or on helium nanodroplets exposed to EUV radiation *J. Phys. Chem. A* **117** 4394
63. Briant M, Mengesha E, De Pujo P, Gaveau M A, Soep B, Mestdagh J M and Poisson L 2016 Large amplitude motion of the acetylene molecule within acetylene–neon complexes hosted in helium droplets *Phys. Chem. Chem. Phys.* **18** 16414
64. Tanyag R M P, Jones C F, Bernando C, O'Connell S M O, Verma D and Vilesov A F 2017 In *Cold Chemistry: Molecular Scattering and Reactivity Near Absolute Zero*. Dulieu O and Osterwalder A (eds.) (RSC: London) p 389
65. Mani D, Fischer T, Schwan R, Dey A, Redlich B, van der Meer A F G, Schwaab G and Havenith M 2017 A helium nanodroplet setup for mid and far-infrared spectroscopy using pulsed-free-electron lasers: Vibrational spectra of propargyl alcohol *RSC Adv.* **7** 54318
66. Niman J W, Kamerin B S, Merthe D J, Kranabetter L and Kresin V V 2019 Oriented polar molecules trapped in cold helium nanodropets: Electrostatic deflection, size separation, and charge migration *Phys. Rev. Lett.* **123** 043203
67. Ernst W E and Hauser A W 2021 Metal clusters synthesized in helium droplets: Structure and dynamics from experiment and theory *Phys. Chem. Chem. Phys.* **23** 7553
68. Zhang J and Kong W 2022 Electron diffraction as a structure Tool for charged and neutral nanoclusters formed in superfluid helium droplets *Phys. Chem. Chem. Phys.* **24** 6349
69. Madeja F, Markwick P, Havenith M, Nauta K and Miller R E 2002 Rotationally resolved infrared spectroscopy of H_2- and D_1-formic acid monomer in liquid He droplets *J. Chem. Phys.* **116** 2870
70. Meyer K A E, Davies J A and Ellis A M 2020 Shifting formic acid dimers into perspective: Vibrational scrutiny in helium nanodroplets *Phys. Chem. Chem. Phys.* **22** 9637
71. Das P, Knapp C J and Jäger W 2017 Ro-Vibrational spectroscopy of the formic acid-D_1 monomer embedded in helium nanodroplets *J. Mol. Spectrosc.* **341** 17
72. Raston P L 2022 Helium nanodroplet isolation spectroscopy in an undergraduate teaching laboratory *J. Mol. Spectrosc.* **388** 111676